Optimization of the Current Profile in MHD Generators

R. Ramberger*
University of Innsbruck, Austria

A method is discussed to reduce the extremely high current density at certain ends of the electrodes in a Faraday MHD generator caused by the Hall effect. To begin with, criteria are developed for improving the electric current profile. With the help of these criteria, a variational principle is formulated for numerically obtaining the "optimal" profile for fixed gasdynamic flow. This optimum is compromising between maximal uniformity of the current pattern and the minimal electrode losses. It can be realized by choosing a suitable conductivity profile in the electrodes. The results of the numerical optimization with the finite element method show that it is indeed possible to achieve a reduction of the current concentration, but only to a certain extent, in order to avoid high potential drops in the electrodes.

Nomenclature

B	= magnetic induction
β	= Hall parameter
δ	= thickness of boundary layer
e	= elementary charge
E	= electric field
η	= electrode thickness
φ	= electrostatic potential
h	= parameter in Eq. (20)
H	= magnetic field
H_0	= external magnetic field
j	= current density
J	= total current per meter in z direction
k	= Boltzmann constant
L_x, L_y	= length and height of segment
Λ	= Lagrange multiplier in Eq. (21)
n_-	= electron density
p_-	= electron pressure
P	= pressure tensor
q	= heat flux
r	= position vector (x,y)
ρ	= mass density
ρ_e	= electric charge density
σ	= electric conductivity
T	= temperature
U	= density of internal energy
v	= plasma velocity
V_H	= Hall voltage
$x_{1,2}$	= x,y

I. Introduction

In long-duration experiments, one has to recognize severe electrode problems playing a crucial part in open-cycle combustion MHD generators of the Faraday type.[1-6] Breakdown in the electrode boundary layers[4,7] or between electrodes[1] leads to intense arc discharges, thus damaging the electrodes at those ends where, due to the Hall effect, the current density is extremely high.

This well-known effect of current concentration, which also has the consequence of reducing the generator's efficiency, has been studied by many authors[4,8-14] both theoretically and experimentally. In theoretical descriptions, boundary-layer effects are often neglected but, in fact, they play an important role in this context.[4,5,7,15-18] In particular, the temperature layer which is present in the vicinity of cooled electrodes has a deterimental effect by reducing the conductivity in the plasma sheath near the wall (see, for example, Ref. 19). In this work, we take into account boundary layers, prescribing suitable profiles of the gasdynamic quantities v, T, and ρ (density).

The problem of current concentrations can be alleviated by a finer segmentation of the electrodes. However, in order to avoid interelectrode breakdown, one cannot go too far with it, and the problem of forming many separate circuits with separate leads arises.[19] On the other hand, there exist several treatments aimed at achieving more uniform current distributions by using *resistive electrodes.*[13,20-22] Rosa tested some finite-resistivity electrodes on the MARK VI generator[4] and, recently, experimental optimization techniques were also suggested.[23] Another proposal was made by Llengyel with his "displaced electrodes."[10]

All of these theoretical approaches are based on rather idealized models of the plasma behavior, whereas we will take boundary-layer effects into full account and also treat the whole problem more rigorously, asking for *optimization criteria* as the basis of a mathematical formulation. The functional we will choose (see Eq. 20) is the generator power plus the square of the axial electric field at the electrode-plasma interface (for details see Sec. II.D). To achieve the "optimal" current distribution in a typical linear duct segment, we follow an idea of Deutsch and Cap,[22] choosing a suitable conductivity profile in the electrodes. The whole problem is solved numerically using the finite element method.

Formally, we use a diffuse-discharge model of a steady-state Faraday generator in thermal equilibrium,[3] which is frequently encountered in literature,[8-12,19] but often much simpler models are used.[14,20,22,24] In addition, in order to include arc-mode transport to some extent, it is possible to

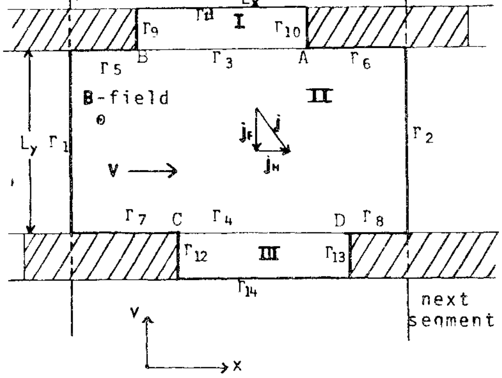

Fig. 1 Model geometry.

Received Aug. 9, 1977; revision received March 7, 1978.
Index category: MHD.

*Scientist.

introduce effective, empirical transport quantities in the arcing regions. Since the mechanism of microarc formation is not completely elucidated today,[7] this seems to be a good approach in theoretical desciption.

The main purpose of this paper is to discuss the possibility of *influencing the current distribution in the channel by an appropriate electrode conductivity profile*. For this purpose, it is adequate to use a diffuse-discharge model. The arcs may then be expected to be distributed more randomly over the whole electrode surface, for real generators exhibiting the "uniform" current density discussed herein. Thus, in particular, the arc damage of the downstream end of the cathode and on the upstream end of the anode is removed—which is exactly our goal.

II. Formulation of the Variational Principle

A. Basic Equations

Let us consider a typical segment in the duct of a Faraday MHD generator. It is described by the time-independent MHD equations, combined with Ohm's law[24] and Maxwell's equations, where all variables may vary in space

$$-\partial\rho/\partial t \equiv \nabla\cdot(\rho v)=0 \tag{1}$$

$$-\partial v/\partial t \equiv \nabla\cdot(\rho vv)+\nabla\cdot P-\rho_e E-j\times B=0 \tag{2}$$

$$-\partial/\partial t(\tfrac{1}{2}\rho v^2+U)\equiv\nabla\cdot(\tfrac{1}{2}\rho v^2 v+Uv+P\cdot v+q)-j\cdot E=0 \tag{3}$$

$$j=\sigma\left(E+v\times B+\frac{\nabla p_-}{n_-e}-\frac{j\times B}{n_-e}\right) \tag{4}$$

In Ohm's law, we neglected the ion slip, as is justified for combustion generators.[25] Maxwell's equations read:

$$\epsilon_0\partial E/\partial t\equiv\nabla\times H-j=0 \tag{5}$$

$$-\partial B/\partial t\equiv\nabla\times E=0 \tag{6}$$

$$\nabla\cdot B=0 \quad B=\mu_0 H \tag{7}$$

$$\nabla\cdot E=\rho_e \tag{8}$$

In the electrodes, we also need Maxwell's equations in the same form. Ohm's law in the electrodes will be assumed to have the simple form

$$j_{\text{el.}}=\sigma_{\text{el.}}E \tag{4a}$$

which is adequate if the electrode Hall parameter is sufficiently low. Except for some semiconductors, most electrode materials have this property.[26] The spatially varying electrode conductivity is not given, but is to be determined (cf. Sec. III. B).

Inserting Eq. (5) into Eq. (4), we get the following expression for E:

$$E=-v\times B+1/\sigma[\nabla\times H]-\frac{\nabla p_-}{n_-e}+\frac{[\nabla\times H]\times B}{n_-e} \tag{9}$$

Taking the curl of Eq. (9), we obtain the induction equation, Eq. (6), for the plasma in the form

$$\nabla\times(\mu_0 H\times v)+\nabla\times\left[\frac{1}{\sigma}\nabla\times H\right]-\nabla\frac{1}{n_-e}\times\nabla p_-$$
$$+\nabla\times\left[\frac{\mu_0}{n_-e}(\nabla\times H)\times H\right]=0 \tag{10}$$

B. Decoupling of the MHD Equations

We assume σ, n_-, p_-, P, U and q to be known functions of plasma density and temperature. So ρ, v, and T are the basic gasdynamic quantities we need. For sufficiently low energy extraction, it is reasonable to expect that the influence of the *specific form* of the current distribution on those gasdynamic profiles is small.[9,19] Raeder discusses this neglect of MHD effects in more detail (pp. 62 and 85 of Ref. 19). In this case, the current distribution can be calculated to a good approximation without solving the MHD equations simultaneously. This procedure is called *decoupling*. As we will consider just one segment in the middle of the MHD channel (see Fig. 1), the ratio of the extracted power to the total energy flux will be small[27] and decoupling is justified.

We want to single out the influence of the electrode conductivity on the current distribution and examine how to thereby reduce the current concentration. The interaction with gasdynamics is not essential in this context, so we will prescribe adequate profiles of ρ, v, and T being consistent with the MHD equations for some suitable (zero-order) electromagnetic field.

With these assumptions, the only unknown in Eq. (10) is H. Together with Eq. (7) and appropriate boundary conditions, Eq. (10) determines $H(r)$.

C. Geometry and Boundary Conditions

As previously stated, we consider only one typical segment in the middle of a linear MHD generator. The boundaries are denoted by Γ_1 through Γ_{14}, the top electrode (anode) by I, the bottom electrode (cathode) by III, and the channel segment by II. Consecutive electrodes are assumed to be separated by insulating wall segments (Fig. 1).

We now make the following usual assumptions which are frequently encountered in literature in similar context.[8,9,19,22]

1) Two-Dimensional Geometry

$$\partial/\partial z=0 \tag{11a}$$

$$j_z=0 \tag{11b}$$

$$H_x=H_y=B_x=B_y=0 \tag{11c}$$

By these assumptions, Eq. (7) is automatically statisfied. Note that further on we will not refer explicitly to the two-dimensional geometry, but take the polar vectors j, E, v, and ∇ as two-dimensional vectors and write H or B just for their z components. Thus the inudction equation, Eq. (10), has only a z component:

$$\mathfrak{D}(H)\equiv(\nabla\cdot v)\mu_0 H+\mu_0 v\cdot\nabla H-\nabla\cdot\left(\frac{1}{\sigma}\nabla H\right)$$
$$-\nabla\frac{1}{n_-e}\times\nabla p_- -\nabla\frac{1}{n_-e}\times(\mu_0 H\nabla H)=0 \tag{12}$$

Our only unknown functions are H (in the whole domain) and σ in the electrodes. Equation (12) contains all the information on our basic plasma equations, Eqs. (1-8).

2) Fixed Boundary Conditions

By Maxwell's equation (5), the magnetic field must be constant along any insulating wall (i.e., on $\Gamma_{5\text{-}10,12,13}$). Furthermore, we require the net electric current through Γ_1 and Γ_2 to vanish so that

$$H=H_0 \quad \text{on} \quad \Gamma_{5,7,9,12}$$
$$H=H_0+J \quad \text{on} \quad \Gamma_{6,8,10,13} \tag{13}$$

At the end points of the electrode-plasma interface (points A-D in Fig. 1), the tangential electric field E_x must be continuous. But since on the electrode side no electric current can flow through Γ_9, etc. (insulator!), E_x must vanish there because of Ohm's law, Eq. (4a). Thus, on the plasma side

$$H_{,x} = \frac{1}{\beta} H_{,y} - \frac{p_{-,x}}{B} \qquad \left(\beta = \frac{\sigma B}{n\_e}\right) \tag{14}$$

must be valid at these points.

3) Quasiperiodic Boundary Conditions

If we neglect end effects, which is justified in the middle of the channel, we may assume that the plasma conditions do not vary significantly from one segment to the next. Thus we can impose periodic boundary conditions for j:

$$j(\Gamma_1) = j(\Gamma_2) \;\text{ or }\; \nabla H(\Gamma_1) = \nabla H(\Gamma_2) \;\text{ for all } y \tag{15a}$$

However, as the net current J is extracted over the electrodes, H itself must satisfy the relationship

$$J + H(\Gamma_1) = H(\Gamma_2) \;\text{ for all } y \tag{15b}$$

Along Γ_3 and Γ_4 no conditions have been imposed so far. This freedom is used to optimize the current distribution.

D. Optimization

In the following sections we work out a procedure intended to provide a conductivity profile in the electrodes which is, in some sense, optimal. The optimization criteria are as follows.

1) The current concentration must be reduced. However, an ideally uniform current distribution along Γ_3 and Γ_4 may give rise to undesired effects on performance, either in the plasma or in the electrodes, which may result in a decrease of the efficiency.

2) Therefore, we must also consider the aspect of global energy conversion. This means that, for fixed total current J, the generated power should be as high as possible.

The first requirement is essentially satisfied by maximizing the net power production *in the plasma*,

$$-\iint_{\mathrm{II}} j \cdot E \; \mathrm{d}x\mathrm{d}y = \max \tag{16}$$

Given $J = \int_0^{Lx} j_y \mathrm{d}x$, the Ohmic losses, being proportional to j^2, increase with increasing current concentration,[27] thus reducing the net power production. The computer results (Fig. 5) confirm this plausibility argument and therefore would justify the use of Eq. (16).

At first sight, the second requirement seems to be satisfied automatically by Eq. (16), but we have to keep in mind that the electrode losses must also be taken into account. If σ_{EI} were much greater than σ_{PI}—which is the case for metallic electrodes—this contribution would be negligible. However, we must expect very low conductivities in the part of the electrodes where the current concentration usually occurs.[13,22] In fact, only optimizing according to Eq. (16) would lead to great potential differences along interfaces Γ_3 and Γ_4, as shown in Fig. 5. One can understand this effect with the help of Ohm's law. Taking

$$|j_x| \ll |j_y| \tag{17}$$

(as a result of the minimization), $\beta \sim 1$ and neglecting the axial gradient of p_-, one would obtain

$$\sigma E_x - \beta j_y \approx 0 \tag{18}$$

Thus, the compensation of the Hall field would require a large potential drop along the electrode wall because of the low σ in the boundary layer adjacent to the electrode. Since on the side where the current is tapped from the electrode the potential must be constant, about the same high-potential drop would also occur *across* the electrode (see Fig. 3b), leading to high losses. *The two requirements just formulated are therefore conflicting with one another.*

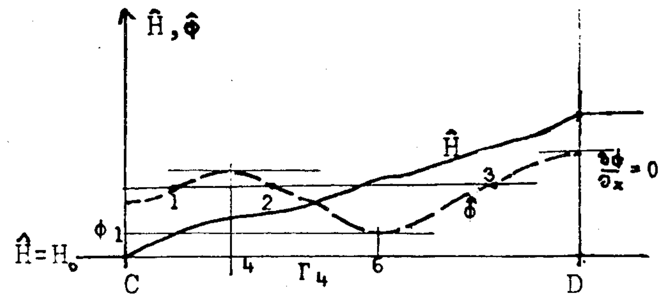

Fig. 2 **A possible distribution of the potential $\hat{\varphi}$ and magnetic field $\hat{H}$ along Γ_4. Points 1,2,3 have the same potential. At C and D, $\hat{H}$ has a discontinuous derivative.**

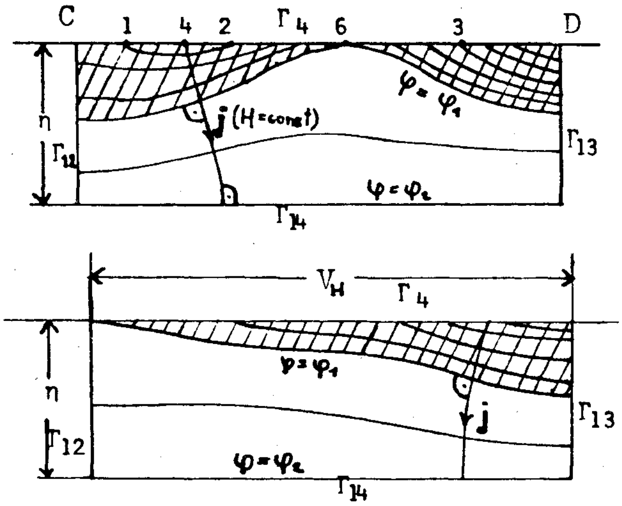

Fig. 3 **a) The equipotential lines in the electrodes. Division into two parts by the line $\varphi = \varphi_1$. The numbered points correspond to Fig. 2. b) The same for monotonic $\hat{\varphi}$ along Γ_4. V_H is the potential difference between C and D.**

As a first expedient, one would think of a variational of the form

$$\iint_{\mathrm{I} \cup \mathrm{II} \cup \mathrm{III}} j \cdot E \; \mathrm{d}x\mathrm{d}y = \min \tag{19}$$

(This integral can be carried out to give $-J.V_G$, where V_G is the voltage between Γ_{11} and Γ_{14}.) However, because in regions I and III σ is also considered unknown, this principle would lead, on one hand, to rather complicated mathematical and numerical problems. On the other hand, the electrode losses do not essentially depend on the specific current and potential distribution, provided that the current is not too far from being uniform. So the losses depend mainly on the *magnitude* of the potential drop across the electrode, which, in turn, is of the order of the Hall voltage V_H along Γ_3 and Γ_4. (In most cases, the resulting potential distribution in the electrodes is monotonic along Γ_3 and Γ_4, respectively, as shown in Fig. 3b. As one can keep the difference $|\varphi_1 - \varphi_2|$ very low by choosing a high conductivity between these two equipotential lines, the mean potential drop between Γ_4 and Γ_{14} is about $V_H/2$—see also Sec. III. B.)

Furthermore, for the construction of a reasonable conductivity profile in the electrodes, the equipotential lines should be as smooth as possible. Therefore, the local E_x

component also has to be kept within bounds. Thus, we finally combine the two requirements from above, adding to Eq. (16) a penalty term which gives a much simpler problem than Eq. (19):

$$\iint_{\mathrm{II}} \boldsymbol{j}\boldsymbol{\cdot}\boldsymbol{E}\ \mathrm{d}x\mathrm{d}y + h\oint_{\Gamma_3\Gamma_4} E_x^2 \mathrm{d}x = \min_{\mathrm{H}}$$

$$\text{(subject to } \mathfrak{D}(H)=0) \tag{20}$$

with $h>0$ as a parameter. The optimization is to be carried out by varying H in such a way that Eq. (12) is fulfilled as a constraint. The choice of h stresses the importance of limiting the Hall field along the interfaces more or less—thus reflecting the compromise between the two requirements just mentioned. A reasonable choice would be $h \simeq 1$ (Fig. 4).

III. Formal Solution

According to the previous discussion, we are now in a position to develop the following procedure.

1) Prescribing no condition along Γ_3 and Γ_4, one is free to vary the current distribution or, equivalently, H in region II in such a way that the induction equation, Eq. (12), is fulfilled. To reduce the current concentration at the electrode edges, it would be sufficient to extremize according to Eq. (16). This, however, would lead to high electrode losses, so that we finally use Eq. (20) as our variational principle.

2) To realize the current distribution which minimizes Eq. (20), we will choose a suitable conductivity profile in the electrodes; this procedure is treated in Sec. III. B. The losses in the electrodes are no longer explicitly minimized by this procedure since they have already been taken into account in formulating Eq. (20).

A. Existence of a Solution of the Variational Principle

To make sure that the induction equation, Eq. (12), is satisfied, we implement it as a constraint with a Lagrange parameter $\Lambda(x,y)$. Thus the complete form of our variational principle is

$$\iint_{\mathrm{II}} \mathrm{d}x\mathrm{d}y\{\boldsymbol{j}\boldsymbol{\cdot}\boldsymbol{E} - \Lambda\mathfrak{D}(H)\} + h\oint_{\Gamma_3\Gamma_4} \mathrm{d}x\ E_x^2 = \underset{H,\Lambda}{\mathrm{stat}} \tag{21}$$

One can show that for "reasonable" functions $\sigma(\boldsymbol{r})$ and $\boldsymbol{v}(\boldsymbol{r})$, the left-hand side of Eq. (21) is positively definite with respect to H.[27] Hence, this variational principle indeed yields a minimum, and this minimum is uniquely determined by Eq. (21), together with the boundary conditions Eqs. (13-15). Expressing $\boldsymbol{E}$ by Ohm's law as in Eq. (9) and substituting $\boldsymbol{j} = \nabla \times \boldsymbol{H}$ we explicitly get for Eq. (21):

$$I \equiv \iint_{\mathrm{II}} \mathrm{d}x\mathrm{d}y\ F(H,\Lambda) + h\oint_{\Gamma_3\Gamma_4} \mathrm{d}x\ E_x^2(H) = \underset{H,\Lambda}{\mathrm{stat}} \tag{22}$$

where

$$F = -(\boldsymbol{v}\boldsymbol{\cdot}\nabla H)\mu_0 H + 1/\sigma(\nabla H)^2 - \frac{1}{n_-e}\nabla p_- \times \nabla H + \Lambda\mathfrak{D}(H) \tag{23a}$$

and

$$E_x = \frac{1}{\sigma}\frac{\partial H}{\partial y} - \frac{1}{n_-e}\frac{\partial p_-}{\partial x} - \frac{\mu_0}{n_-e}H\frac{\partial H}{\partial x} \quad \text{along } \Gamma_3,\Gamma_4 \tag{23b}$$

The appropriate boundary conditions are Eqs. (13-15). As just stated, Γ_3 and Γ_4 are free boundaries; otherwise H would be completely determined by Eq. (12). Varying H and Λ, we get more boundary conditions in the form of transversality conditions needed to make some surface integrals to vanish:

$$\delta I = \iint_{\mathrm{II}} \mathrm{d}x\mathrm{d}y\Big\{\frac{\partial F}{\partial H}\delta H + \sum_{i=1}^{2}\frac{\partial F}{\partial H_{,x_i}}\delta H_{,x_i} + \sum_{i=1}^{2}\frac{\partial F}{\partial H_{,x_ix_i}}\delta H_{,x_ix_i} + \frac{\partial F}{\partial \Lambda}\delta\Lambda\Big\} + h\oint_{\Gamma_3\Gamma_4}\mathrm{d}x . 2E_x\Big\{\frac{1}{\sigma}\delta H_{,y} - \frac{\mu_0}{n_-e}(H\delta H_{,x} + H_{,x}\delta H)\Big\} = 0 \tag{24}$$

Integrating by parts, we obtain

$$\delta I = \iint_{\mathrm{II}} \mathrm{d}x\mathrm{d}y\Big\{\frac{\partial F}{\partial H}\delta H - \sum_i \frac{\partial}{\partial x_i}\Big(\frac{\partial F}{\partial H_{,x_i}}\Big)\delta H + \sum_i \frac{\partial^2}{\partial x_i^2}\Big(\frac{\partial F}{\partial H_{,x_ix_i}}\Big)\delta H + \frac{\partial F}{\partial \Lambda}\delta\Lambda\Big\}$$
$$+ \oint \mathrm{d}x_t\Big\{\frac{\partial F}{\partial H_{,x_n}}\delta H - \frac{\partial}{\partial x_n}\frac{\partial F}{\partial H_{,x_nx_n}}\delta H\Big\} + 2h\oint \mathrm{d}x\Big(E_x\frac{1}{n_-e}\Big)_{,x}\mu_0 H\delta H + \oint \mathrm{d}x_t \frac{\partial F}{\partial H_{,x_nx_n}}\delta H_{,x_n}$$
$$+ 2h\oint_{\Gamma_3\Gamma_4}\mathrm{d}x E_x\frac{1}{\sigma}\delta H_{,y} = 0 \tag{25}$$

where x_t, x_n denote the tangential, respectively normal coordinate.

So we have the Euler-Lagrange equations

$$\frac{\partial F}{\partial H} - \frac{\partial}{\partial x}\frac{\partial F}{\partial H_{,x}} - \frac{\partial}{\partial y}\frac{\partial F}{\partial H_{,y}} + \frac{\partial^2}{\partial x^2}\frac{\partial F}{\partial H_{,xx}} + \frac{\partial^2}{\partial y^2}\frac{\partial F}{\partial H_{,yy}} = 0 \tag{26}$$

$$\frac{\partial F}{\partial \Lambda} = 0 \tag{27$\equiv$(12)}$$

and the following transversality conditions:

1) From the last two integrals:

$$\Lambda = 0 \quad \text{on} \quad \Gamma_{5,6,7,8} \tag{28a}$$

$$\Lambda \pm hE_x/\sigma = 0 \quad \text{on } \Gamma_3(+) \text{ and } \Gamma_4(-) \tag{28aa}$$

with Eq. (15a) we get from the rest of the fourth integral

$$\Lambda/\sigma\,|_{\Gamma_2,y} - \Lambda/\sigma\,|_{\Gamma_1,y} = 0 \tag{28b}$$

2) From the second and third integrals:

$$\frac{\partial F}{\partial H_{,y}} - \frac{\partial}{\partial y}\frac{\partial F}{\partial H_{,yy}} \pm 2h\Big(\frac{E_x}{en_-}\Big)_{,x}\mu_0 H = 0 \tag{28c}$$

and with Eq. (15b) we get from the rest of the second integral

$$\Big[\frac{\partial F}{\partial H_{,x}} - \frac{\partial}{\partial x}\frac{\partial F}{\partial H_{,xx}}\Big]_{\Gamma_1} - \Big[\frac{\partial F}{\partial H_{,x}} - \frac{\partial}{\partial x}\frac{\partial F}{\partial H_{,xx}}\Big]_{\Gamma_2} = 0 \tag{28d}$$

Equation (27) is evidently of the elliptic type. Writing Eq. (26) explicitly, one can see that this is an elliptic equation for Λ. Thus, these two coupled equations have a unique solution if one takes the boundary and transversality conditions into account.

B. Conductivity Profile in the Electrodes

Suppose we now have found the solution of the variational problem Eq. (22). To realize the boundary values on Γ_3 and Γ_4 which result from this solution, we have to choose a suitable conductivity profile in the electrodes. As we will see, this choice is not unique, but for our goal—to reduce the current concentration—it is not so important what the specific distributions look like, provided that 1) the boundary conditions in Eqs. (29) and (30) are satisfied; and 2) they are not too far from being uniform (c.f., Sec. II.D). This requirement is achieved by the following procedure, as the results show.

To be specific, we take the lower electrode (cathode), but the following considerations analogously apply to the upper electrode.

Because of the conditions in Eq. (13) on Γ_{12} and Γ_{13}, the normal component of $\boldsymbol{E}$ must vanish, i.e.,

$$\partial\varphi/\partial x=0 \quad H=\begin{cases} H_0 & \text{on } \Gamma_{12} \\ H_0+J & \text{on } \Gamma_{13} \end{cases} \tag{29a}$$

where φ is the electrostatic potential.

On Γ_{14} the electrodes may border on a conductor of very high conductivity so that

$$j_x=\partial H/\partial y=0 \quad \varphi=\text{const}=\varphi_2 \text{ on } \Gamma_{14} \tag{29b}$$

The normal current distribution j_y along Γ_{14} need not be fixed. We will get some distribution of H (and so of $j_y=-\partial H/\partial x$) along Γ_{14} as a result of our calculations. We may suppose that it is possible in principle to obtain this distribution by suitably arranging external leads.

On Γ_4, $\boldsymbol{E}_t$ and, because of the absence of surface currents,[8] $\boldsymbol{H}_t$ must also be continuous:

$$H(\Gamma_4,\text{el.})=H(\Gamma_4,\text{pl.})\doteq\hat{H}(x)$$

$$\varphi(\Gamma_4,\text{el.})=\varphi(\Gamma_4,\text{pl.})\doteq\hat{\varphi}(x) \tag{30}$$

Employing Ohm's law, Eqs. (4a) and (5), we have in our two-dimensional geometry:

$$\nabla\varphi\cdot\nabla H=-1/\sigma \quad j\cdot\nabla H=0 \tag{31}$$

Thus, the gradients of φ and H and, in addition, the lines of constant φ and H are perpendicular to one another, it is mainly a geometrical problem to find some suitable H and φ lines. Of course, there is some arbitrariness in this problem because we have only one Eq. (31) for two unknowns (H and φ), except for the boundary conditions.

We may assume that, in the optimal case, there is no point along the interface Γ_4 where the current flows from the cathode back into the plasma. Therefore, by virtue of Eq. (5), H increases monotonically with x. On the other hand, the potential need not necessarily be monotonic (cf., Fig. 2), though it seems to be in most cases.

Solving Eq. (31), lines $\varphi=$const and $H=$const are the characteristics for φ and H, respectively. Now, because of the possible nonmonotonic behavior of φ, there can exist characteristics for φ which intersect with Γ_4 (where φ is given) more than once (see Figs. 2 and 3a). To overcome this difficulty, we prescribe first a consistent φ distribution, satisfying all boundary conditions, Eqs. (29) and (30), and then calculate H as the solution of Eq. (31) with the boundary condition, Eq. (30). This solution is obtained just by putting $H=$const along the characteristics. (Note that the boundary conditions, Eqs. (29) for H are then automatically fulfilled.

Looking for a suitable φ distribution, one can see that the potential drop in the electrodes can be kept as low as possible by choosing φ_2 so that $\varphi_1-\varphi_2$ is very low. Here, φ_2 is the potential on Γ_{14} and φ_1 its minimum along Γ_4 (Fig. 3a). For simplicity, we use for φ:

$$\bar{\varphi}(x,y)=\hat{\varphi}(x)-\frac{y-\hat{y}}{\eta}[\bar{\varphi}_2-\hat{\varphi}(x)] \quad \bar{\varphi}_2=\varphi_1+\frac{\varphi_2-\varphi_1}{1-a}$$

$$\varphi(x,y)=\begin{cases} \bar{\varphi}(x,y) & \text{if } \bar{\varphi}\geq\varphi_1 \\ (1-a)\bar{\varphi}(x,y)+a\varphi_1 & \text{if } \bar{\varphi}<\varphi_1 \end{cases} \quad 1>a\geq 0 \tag{32}$$

where η is the electrode thickness and $\hat{}$ indicates the value on Γ_4. The parameter a is used to arbitrarily varying the difference $\varphi_2-\varphi_1$. Choosing $a=1-\epsilon$ is equivalent to a scaling of the conductivity in the region between $\varphi=\varphi_1$ and $\varphi=\varphi_2$ with the factor $1/\epsilon$, because on scaling, the shape of the current and equipotential lines remains unchanged.

One can easily see that the ansatz, Eq. (32), satisfies all boundary conditions Eqs. (29) and (30). Constructing now the orthogonal trajectories to the lines $\varphi=$const (which are equivalent to $\bar{\varphi}=$const), one gets the lines $H=$const (characteristics), and so the magnetic field in the whole electrode (domain III)[27]:

$$H(x,y)=\hat{H}(\hat{x}(x,y)) \tag{33}$$

$\hat{x}(x,y)$ is the coordinate of the point of intersection between the characteristic through (x,y) and Γ_4 with $\hat{H}(x)$ defined in Eq. (30). The characteristics can be found in the usual way, and the integrals involved have rational integrands.

Finally, the electric conductivity can be calculated with Ohm's law:

$$1/\sigma(x_A,y_A)=\left.\frac{\varphi_{,y}}{H_{,x}}\right|_{x_A,y_A} \quad \text{at any point } (x_A,y_A) \tag{34}$$

Inserting for φ from Eq. (32) and taking into account that

$$\left.\frac{\partial H}{\partial x}\right|_{x_A,y_A}=\left.\frac{\mathrm{d}\hat{H}}{\mathrm{d}x}\right|_{\hat{x}}\cdot\left.\frac{\partial\hat{x}}{\partial x}\right|_{x_A,y_A}$$

one gets, after some algebra,[27]

$$1/\bar{\sigma}(x_A,y_A)=\frac{|\hat{\varphi}(\hat{x})-\bar{\varphi}_2|}{\eta\mathrm{d}\hat{H}/\mathrm{d}x|_{\hat{x}}}\cdot\frac{\mathrm{d}\hat{\varphi}/\mathrm{d}x|_{x_A}}{\mathrm{d}\hat{\varphi}/\mathrm{d}x|_{\hat{x}}}$$

and

$$1/\sigma=\left\{\begin{matrix} 1/\bar{\sigma} & \text{if } \bar{\varphi}\geq\varphi_1 \\ \dfrac{1-a}{\bar{\sigma}} & \text{if } \bar{\varphi}<\varphi_1 \end{matrix}\right\} \text{ at the point } (x_A,y_A) \tag{35}$$

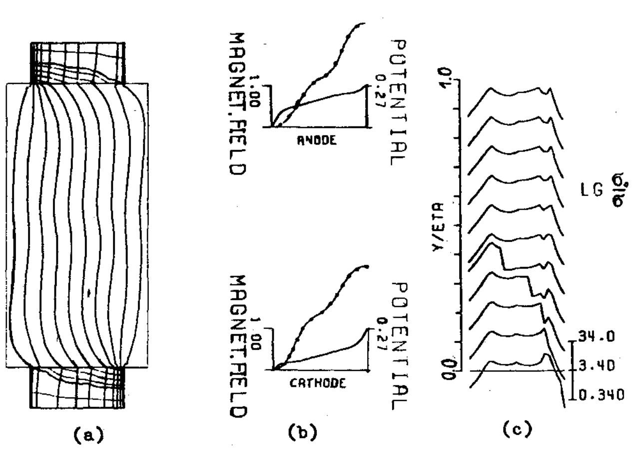

Fig. 4 a) Current and potential distribution for the first example, b) Variation of H (——) and φ (—·—) along Γ_3 and Γ_4; c) Resistivity distribution in the anode.

Thus, we have shown a possible construction of a "suitable conductivity profile" in order to reduce the current concentration and to make the losses minimal—in the sense discussed in deriving the variational principle Eq. (20).

IV. Results

To illustrate the method discussed here, a few special results are presented. For convenience, in these examples, the gasdynamic profiles were assumed to be independent of x, which is reasonable, since we are considering just one segment in the middle of the channel. But this is not to be regarded as a restriction to the method, because arbitrary profiles could be implemented straightforward, if necessary, e.g., for introducing effective transport quantities in the arcing region mentioned in the introduction. The particular profiles within a boundary layer of thickness δ were chosen close to those given by Raeder,[19] where MHD effects have been taken into account to some extent:

$$v_y = 0 \quad v_x = \left|\frac{y - y_{\text{wall}}}{\delta}\right|^{1/r_1} v_0 \quad r_1 \cong 7$$

$$p_- = n_- kT \quad n_- = n_{-0}\exp[-b/T_0(T/T_0 - 1)](T/T_0)^c \tag{36}$$

where n_{-0}, T_0 are the density and temperature of the core plasma, $b \simeq -2000$ deg and $c \simeq 8$;

$$\sigma \propto n_- T^{r_2} \quad r_2 \simeq 1$$

$$T = T_{\text{wall}} + (T_0 - T_{w.})\left|\frac{y - y_{w.}}{\delta}\right|^{1/r_3} \quad r_3 \simeq 9 \tag{37}$$

The solution of the variational problem Eq. (22), was carried out on a computer using the finite element method.[28] The coefficients in F and E_x in Eq. (22), as well as the unknown function H, were expressed by hermite bicubic splines.[27,28] This was necessary in order to also obtain the derivatives to a good approximation. After calculating the distribution of H and derivatives in region II and at interfaces Γ_3 and Γ_4 by this procedure, the code calculates φ, H, and $1/\sigma$ in the electrode regions with the method discussed in the preceding section.

Figure 4 shows the result for a typical test generator with the following parameters:

$$L_y = 0.20\,\text{m} \quad \sigma_0 = 10\,\text{mho/m} \quad T_0 = 2500\text{K} \quad T_{w.} = 2000\text{K}$$

$$L_x = 0.10\,\text{m} \quad v_0 = 1000\,\text{m/s} \quad B_0 = 5\,\text{T} \quad \beta_0 = 2$$

where the subscript "0" indicates the central streaming properties. For the parameters just listed we use:

$$r_1 = 6.38 \quad r_2 = 1.0 \quad r_3 = 9.5$$

$$b = -2000\,\text{deg} \quad c = 7.5 \quad \delta = 0.1$$

In the electrodes, we take

$$(\text{thickness})\eta = 0.2L_x \quad \text{length} = \tfrac{2}{3}L_x \quad a = 0.8 \text{ in Eq. (32)}$$

Figure 4a shows the current lines and also the equipotential lines in the electrodes—the electrodes are plotted on an extended scale in the y direction just to demonstrate the structure of φ and H inside. Figure 4b shows the variation of $(H - H_0)/J$ and $\varphi\sigma_0/J$ (referred to the left end) along interfaces Γ_3 and Γ_4, respectively. Figure 4c gives the calculated distribution of σ_0/σ in the anode on a logarithmic scale. For eleven cuts through the electrode along x—for y fixed—the x axis is shifted each time, as indicated on the left-hand side. The profile in the cathode is practically symmetric to that, because of our simplified assumptions on symmetric gasdynamic profiles.

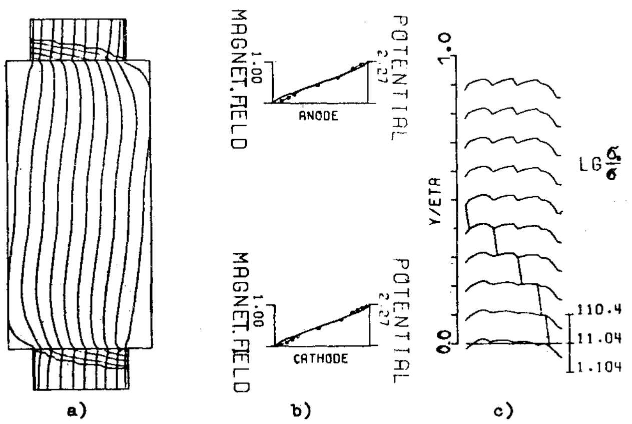

Fig. 5 Current and potential distribution without using the penalty term.

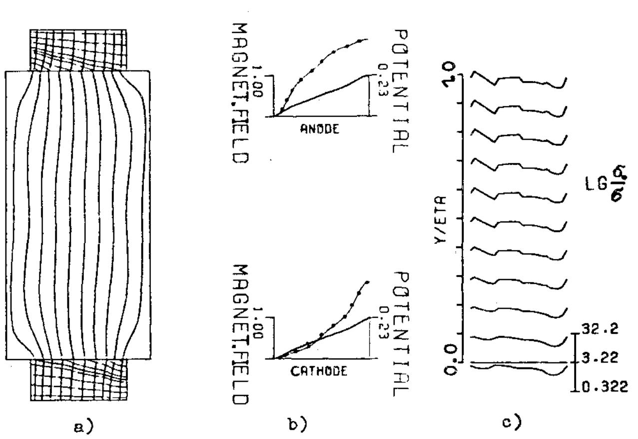

Fig. 6 Current and potential distribution for a Hall parameter reduced to a quarter.

To illustrate the effect of the penalty term in Eq. (20), an example, without using that term, is shown in Fig. 5. All the other parameters are equal to those just mentioned, except $a = 0.9$. One can immediately see that the current lines are more uniform than in Fig. 4, but the potential differences along the interfaces are much higher, and, as a result, the resistance of the electrodes is also heavily increased. The ratio of the total resistances in the electrodes and in the plasma is roughly

$$\frac{2R_{\text{el.}}}{R_{\text{pl.}}} \approx \frac{2\overline{\Delta\varphi}\sigma_0}{1.1JL_y/L_x} \tag{38}$$

where $\overline{\Delta\varphi}$ is the mean potential drop in one electrode. This ratio becomes about 1 in this example, whereas it is about ¼ in the first example.

Figure 6 demonstrates very clearly the role of the Hall effect. The Hall parameter in the core was chosen as $\beta_0 = 0.5$, while the other parameters except a, agree with the first example. (For comparison, we chose $a = 0$, to also have an example in which the conductivity in the electrode regions between $\varphi = \varphi_1$ and $\varphi = \varphi_2$ was not scaled—cf., Eq. 32.) One can see that the current concentration has nearly disappeared, but the potential drop is also slightly reduced in comparison to Fig. 4. Of course, the resistivity of the electrodes is also lower.

Discussion

It is evident that it is really possible to reduce the current concentration a great deal with appropriate resistive electrodes and, simultaneously, keep the potential drops in the electrodes within bounds. In the first example, the resulting resistivity is higher in the middle (Fig. 4c), while, in the last case, it is slightly increasing toward the left end (Fig. 6c). Unfortunately, one also has to take into account numerical errors of about 20%, because of limited computer core (32K) and time available. Therefore, no general conclusions on the necessary conductivity profile can be drawn at this stage.

There seems to be little influence of our resistive electrodes on the conversion efficiency if one includes electrode losses. In a rough estimate, where the author compared the first example (Fig. 4) with the case of constant high-σ electrodes and the same gasdynamic parameters, one can expect that the reduction of the Ohmic losses in the plasma slightly surmounts the additional losses in the electrodes. However, it is doubtful if such a direct comparison has much relevance. For a definite answer, our electrodes had to be tested experimentally.

V. Summary and Conclusions

Considering a typical duct segment in the middle of a linear MHD generator, we looked for a solution of the induction Eq. (12) that should provide a reduction of the current concentration on the electrode edges, as well as good conversion properties. To do so, we optimized the functional Eq. (20) where h was a weight parameter which related these demands. We saw that the choice of h reflects the compromise which is necessary in order for the total resistance of the electrodes to remain low.

To realize the optimal current distribution which was calculated numerically, we suggested to choose a suitable conductivity profile in the electrodes. This should provide the proper boundary conditions on the electrode-plasma interfaces.

Already the few results presented here clearly show that it is indeed possible to reduce the current concentration and therefore to increase the lifetime of the electrodes. Thus, our main goal has been achieved, whereas the question of conversion efficiency has not been treated in detail here, but it is expected that the corresponding difference between our result and a constant-σ-electrode generator is slight.

Thus from these and some other results where the parameter h in Eq. (20) was varied, one can conclude that *it is possible to homogenize the current distribution to some extent, applying suitable resistive electrodes, but it does not seem to be possible to simultaneously increase the conversion efficiency essentially.*

Acknowledgment

The author is indebted to F. Cap for suggesting and supporting this work. It was his idea to try to improve the current profile by suitable resistive electrodes. The author wants likewise to express his gratitude to S. Kuhn and R. V. Deutsch for many helpful discussions. This work was financially supported by the Scientific and Industrial Austrian Research Councils.

References

[1] Oliver, D. A., "Inter-Electrode Breakdown on Electrode Walls Parallel and Inclined to the Magnetic Field," *Proceedings of the 6th International Conference on MHD Electric Power Generation*, Vol. I, Washington, D.C., June 1975, pp. 329-343.

[2] "MHD Electric Power Generation," 1972 and 1976 Status Reports, NEA/IAEA 1973 and 1977.

[3] Sheindlin, A. E. and Jackson, W. D., "MHD Electric Power Generation—An International Status Report," World Energy Conference, Detroit, 1974.

[4] Rosa, R., Petty, S., and Enos, G., "Long Duration Testing in the MARK VI Facility," *Proceedings of the 14th Symposium on Engineering Aspects of MHD*, University of Tennessee Space Institute, April 1974, Paper 1.5.

[5] Petty, S., Rosa, R., and Cole, J., "Developments with the MARK VI Long-Duration MHD Generator," *Proceedings of the 6th International Conference on MHD Electric Power Generation*, Vol. I, Washington, June 1975, pp. 231-249.

[6] Vasil'ev, N. N., et al., "Arc Processes in MHD Generators," *Proceedings of the 6th International Conference on MHD Electric Power Generation*, Vol. I, Washington, June 1975, pp. 359-368.

[7] Messerle, H. K., Campbell, B., and Ho, N. L., "Layer Breakdown on Different Electrode Materials," *Proceedings of the 6th International Conference on MHD Electric Power Generation*, Vol. I, Washington, June 1975, pp. 389-398.

[8] Cap, F., et al., "Stromdichteverteilungen an MHD-elektroden," Institut für Theoretische Physik der Universität Innsbruck, Austria, UNICP-JGC 74 and UNICP-HGC 72.

[9] Fritzer, P., "Simultane Numerische Berechnung 2-dim. MHD-Strömungen," Dissertation, Innsbruck 1972, and *Elektrotechnik & Maschinenbau*, Vol. 1974/2, pp. 73-84.

[10] Lengyel, L., "Current and Potential Distribution in MHD-Generators," Max-Planck-Institut für Plasmaphysik, Rept. IPP-3/50, Garching 1966.

[11] Argyropoulos, S., Casteel, M., and Demitriades, S., "2D Distribution of Current Along MHD-Channels," *Proceedings of the 10th Symposium on Engineering Aspects of MHD*, MIT, Cambridge, 1969, pp. 29-32.

[12] Uncles, R., "The Numerical Prediction of Streamer Growth," *AIAA Journal*, Vol. 11, 1973, pp. 1436-1438.

[13] Croitoru, Z., "Les generateurs MHD à électrodes semi conductrices," *Proceedings of the International Symposium on MHD Power Generation*, Salzburg, 1966, paper SM-74/70.

[14] Fischer, F., "Experimental Investigation of the Current Density Distribution in a Simulated MHD Generator," *AIAA Journal*, Vol. 6, May 1968, pp. 894-900 and Celinsky, Z., Fischer, F., "Effect of Electrode Size in MHD-Generators with Segmented Electrodes," *AIAA Journal*, Vol. 4, March 1966, pp. 421-428.

[15] Lyubimov, G. A., German, V. O., and Parfenov, B. V., "Experimental Investigation of the Potential-Drop Near the Electrode Surface," *Proceedings of the 11th Symposium on Engineering Aspects of MHD*, Pasadena, 1970, p. 61.

[16] Buznikov, A. F., Vanin, V. E., Kirillov, V. V., and Sokolov, Y. N., "Experimental Investigation of the Influence of Boundary Layers upon Performance on MHD Generators Within a Wide Range of Hall Parameters," *Proceedings of the 5th International Conference on MHD Electric Power Generation*, Vol. I, Munich, 1971, pp. 335-350 and Messerle, H. K., Sakuntala, M., and Fu, T., "Electrode Boundary Layers and Surface Effects," ibidem, Vol. II, pp. 325-339.

[17] Teno, J., Liu, C., and Brogan, T. R., "Boundary Layers in MHD Generators," *Proceedings of the 10th Symposium on Engineering Aspects of MHD*, MIT, Cambridge, 1969, pp. 15-22.

[18] Eustis, R., Cima, R. M., and Berry, K., "Current Distribution in Conducting Wall MHD Generators," *Proceedings of the 11th Symposium on Engineering Aspects of MHD*, Pasadena, 1970, pp. 119-127.

[19] Raeder, J., Bünde, R., "Baureife Unterlagen für einen Verbrennungs-MHD-Generator," Max-Planck-Institut für Plasmaphysik, Rept. IPP N/60, Garching 1973 and Raeder, J., *MHD Power Generation*, Chaps. 2 and 4.2, Springer, Heidelberg, 1975, pp. 5-84 and 136-151.

[20] Rohatgi, V., Jayakumar, R., and Ghosh, S., "Effect of Shape and Resistivity of Electrodes in a Faraday MHD Duct," *Proceedings of the 6th International Conference on MHD Electric Power Generation*, Washington, June 1975, Vol. I, pp. 301-315.

[21] Rosa, R. and Petty, S., "Status Report on the MARK VI," *Proceedings of the 13th Symposium on Engineering Aspects of MHD*, Stanford, 1973, paper II.7.

[22] Deutsch, R., "A Possibility for Providing Uniform Current Pattern...," *Plasma Physics*, Vol. 17, March 1975, pp. 225-236.

[23] Tanaka, D. and Hattori, Y., "Characteristics of Resistive Electrodes in MHD-Generator Duct and a Minimization Technique for Internal Power Losses," *Journal of Nuclear Science-Technology*, Vol. 12/11, 1975, p. 687.

[24] Sutton, G. and Sherman, A., *Engineering MHD*, Chap. 14, McGraw Hill, N.Y., 1965, pp. 471-528.

[25] Kruger, C., Mitchner, M., and Daybelge, K., "Transport Properties of MHD-Generator Plasmas," *AIAA Journal*, Vol. 6, Sept. 1968, pp. 1712-1723.

[26] Busch, G., and Schade, H., *Vorlesungen über Festkörperphysik*, Birkhäuser, Basel, 1973, pp. 380-396.

[27] Ramberger, R., "Optimierung des Stromlinienverlaufes in MHD-Generatoren mit Hilfe variabler Elektrodenleitfähigkeit," Disseration, Universität Innsbruck, Juli 1976.

[28] Strang, G. and Fix, G., *An Analysis of the Finite Element Method*, Prentice Hall, Englewood Cliffs, N.J., 1973.